Colloid & Polymer Science Colloid Polym Sci 272:1363–1372 (1994)

Morphological characterization during deformation of a poly(ether ester) thermoplastic elastomer by small-angle x-ray scattering*)

S. Fakirov[1,4]) Z. Denchev[2]), A. A. Apostolov[2]), M. Stamm[3]), and C. Fakirov[3])

[1]) Bogazici University, Department of Chemical Engineering, Polymer Research Center and TUBITAC Advanced Polymeric Materials Research Center, Bebek, Istanbul, Turkey
[2]) Sofia University, Laboratory on Structure and Properties of Polymers, Sofia, Bulgaria
[3]) Max-Planck-Institut für Polymerforschung, Postfach 3148, Mainz, FRG
[4]) Permanent address: Sofia University, Laboratory on Structure and Properties of Polymers, Sofia, Bulgaria

*) *Dedicated to the 65th birthday of Prof. E.W. Fischer*

Prof. Fischer was always a guide and patient teacher to us, he inspired our work with his intense interest and many valuable suggestions. We want to congratulate and thank him sincerely and extend our best wishes for the future.

Abstract: The scattering behavior of pre-drawn and annealed bristles of a highly deformable poly(ether ester) thermoplastic elastomer based on poly(butylene terephthalate) as hard segments and poly(ethylene glycol) as soft segments in a ratio of 57/43 wt.-% is studied. Small-angle x-ray scattering measurements with an area detector are carried out on bristles with and without application of stress up to 195% relative deformation. Two-dimensional scattering patterns are used for morphological characterization of the sample.

At small deformations one morphology peak is found, corresponding to a periodicity that changes affinely with deformation. The morphology of the sample represents assemblies of mutually parallel crystalline lamellae, positioned perpendicular to the stretching direction both under and without stress. When macrodeformation increases a second peak appears, and a four-point pattern is observed in the relaxed state. In this intermediate deformation range coexisting morphologies contribute to the scattering. Additional contributions arise from lamellae, which are inclined to the stretching direction, as well as from lamellae, which are again perpendicular to the stretching direction, as a result of microfibril relaxation and loss of interfibrillar contacts. At large deformations the latter morphology dominates and the 2D-scattering pattern again shows a two-point character. A morphological model for this behaviour is discussed, where the break of interfibrillar contacts during deformation and the inhomogeneous stress field in the sample play an important role.

Key words: Thermoplastic elastomers – deformation behavior – x-ray scattering – long spacing

Introduction

In recent studies of poly(ether ester) (PEE) thermoplastic elastomer based on poly(butylene terephthalate) (PBT) as hard segments and poly(ethylene glycol) (PEG) as soft segments (PBT/PEG = 49/51 wt.-%) the understanding of the deformation mechanism was attempted. For this purpose the relationship between the external (macro-) deformation ε and the microdeformation (on morphological level expressed by the changes in the long spacing L) was followed within a broad deformation range by means of small-angle x-ray scattering (SAXS) [1–5]. The affine and reversible

increase of L at low macrodeformations (up to ε = 50–75%) is found to be related to reversible conformational changes in the intercrystalline amorphous regions in accordance with previous reports on polyethylene [6, 7] and other thermoplastic elastomers [8–13]. At this level of deformation a second long spacing L_2 appears with value close to the starting one L_1^0 and remains constant up to ε = 200–300% [1–3]. L_2 arises as a result of elimination of interfibrillar contacts and relaxation of some microfibrils [1].

In a subsequent study [4] the morphological changes in drawn and undrawn PEE, being of conventional and increased molecular weight were followed by means of two-dimensional (2D) SAXS patterns [4]. At low macrodeformations no substantial morphological changes occur and the morphology of the drawn samples can be envisaged as assemblies of mutually parallel crystalline lamellae positioned perpendicular to stretching direction (SD). In the absence of external stress after previous deformation the morphology changes towards the formation of zigzag-shaped lamellae, i.e., lamellae within microdomains are inclined with respect to the SD. After loading, they take perpendicular position to the SD and thus smoother assemblies of parallel lamellae are formed. This morphological transition from zigzag to smooth lamellae is found to be reversible and becomes more pronounced with the progress of deformation [4].

It should be noted that the described morphological study was performed only with respect to the first type of long spacings expressed by L_1. The second type of long spacings, i.e. L_2 was poorly resolved or even absent in the 2D-SAXS patterns. For this reason it was not possible to perform similar morphological characterization for the lamellae giving rise to L_2.

Such an opportunity appeared after changing the stabilizer used in the synthesis of PEE. All samples discussed above [1–5], which for convenience in the following text will be referred to as PEE I, are stabilized by means of an oligomer, containing hindered phenolic and secondary amino groups [14]. Using a new phenolstyrene based stabilizer named BFSA-2[15] a PEE (PBT/PEG = 57/43 wt.-%) with improved mechanical properties was obtained. This new material will be further denoted as PEE II. In the undrawn state it reveals a deformation at break up to ε = 1200% (against ε = 600% for PEE I [15]).

It is the aim of this work to characterize the morphological behavior of PEE II and to focus in particular on the change of crystalline lamellae and morphology during intermediate and large deformations by means of 2D-SAXS.

Experimental

The starting material represents a polyblock PEE comprising PBT as hard segments and PEG molecular weight of 1000 and polydispersity of 1.3, according to gel permeation chromatography analysis [1] as soft segments in a ratio of 57/43 wt.-%. The synthesis was carried out on a semicommercial scale as described elsewhere [16]. The BFSA-2 stabilizer was chosen since it leads to the best mechanical properties of PEE in comparison to five other stabilizers keeping at the same time a comparatively high relative viscosity of 1.66 [15]. The sample was shaped as a bristle, drawn at room temperature to five times its initial length, and then annealed with fixed ends for 6 h in vacuum at a temperature of 170 °C.

The SAXS experiments were performed with a pinhole camera on an 18 kW rotating-anode generator using CuK_α radiation and a graphite double monochromator. An area gas detector with 512 × 512 pixels and 0.2 mm spatial resolution in each direction was used and the sample-to-detector distance was set to 123 cm. Each measurement under stress σ was immediately followed by another one in the absence of stress (σ = 0) before applying the next, larger deformation. All 2D patterns were obtained and processed by means of *General Area Detector Diffraction Software* from SIEMENS. They were averaged over four points in a small box to reduce statistical variations. Meridional and azimuthal integration was performed at different azimuthal (χ) and scattering (θ) angles, respectively. The azimuthal scans presented in this paper were taken in the χ-range 0–180° and at scattering angles of maximum intensity for the peaks of interest. Further details on the preparation and the treatment of the sample as well as the conditions of the SAXS measurements can be found in ref. [1]. A meridional integration at χ = 90° for instance thus corresponds to a cut through the detector along a line from the lower to upper middle of the detector (*y*-

direction), and the intensity is then typically averaged over ± 10 pixels in the x-direction. The data are generally corrected for background scattering, detector efficiency, change of sample volume during stretching and counting time. Curves are thus comparable with one another while they are not on an absolute scale.

Results

In Fig. 1 some typical two-dimensional diffraction patterns of PEE II in different deformation states are shown. All experimental graphs represented are derived from 2D patterns by means of radial or circular integration. Thus, the small-angle scattering curves given in Fig. 2 taken at various deformation states of the sample, i.e. with and without application of stress, are obtained as slices through the 2D pattern in the vertical direction, i.e., along the fiber axis. It is seen that the strain affects both the angular position and the intensity of the maxima. Splitting of the peak into two maxima (four-point diagram) is observed after macrodeformations of $\varepsilon = 75\%$ and 100% (Fig. 1e) for relaxed samples. Similarly, for $\varepsilon = 75\%$ and 100% one observes an indication of splitting in meridional direction (Fig. 1b).

The effect of the relative macrodeformation ε on the long spacing L, obtained from Fig. 2 is shown in Fig. 3. The open symbols refer to measurements under stress, whereas the filled ones refer to measurements without application of stress ($\sigma = 0$) after applying a deformation $\varepsilon > 0$. Starting from $L_1^0 = 150$ Å, a large increase of the long spacing (denoted as L_1) with increase of the relative deformation can be observed up to $\varepsilon = 100\%$. At $\varepsilon = 75\%$ and 100% a second long spacing L_2 arises, its value being close to the initial one and remaining the same for the next, larger deformations $\varepsilon = 125\%$ to 195%. At the same time, the corresponding second long spacing, measured without stress drops abruptly to 125 Å. Also, after relaxation the first spacing L_1 relaxes to L_1^{rel} which is close to the initial value at $\varepsilon = 0$ and to L_2.

It is seen that in the deformation range $\varepsilon = 0$–50% the changes of L_1 are completely re-

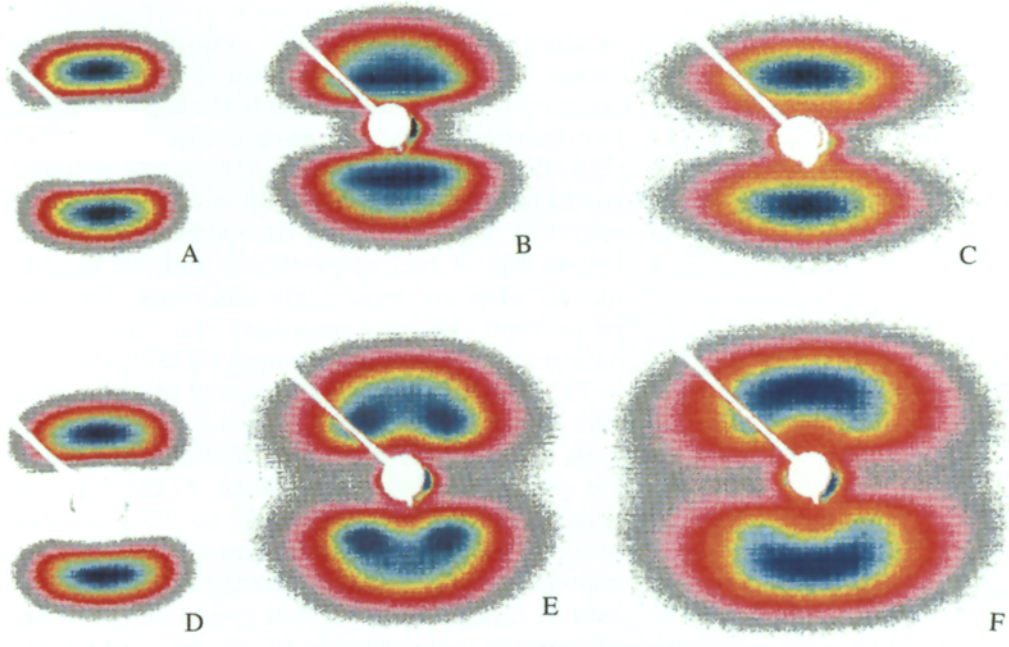

Fig. 1. Selected 2D x-ray diffraction patterns of PEE II representative for the states of deformation investigated. The measurements shown are performed at: a) $\varepsilon = 0\%$ (the sample is previously drawn five times and annealed with fixed ends); b) $\varepsilon = 75\%$; c) $\varepsilon = 195\%$; d) remaining plastic deformation $\varepsilon = 1.5\%$ without stress ($\sigma = 0$) after previous measurement at $\varepsilon = 20\%$; e) remaining plastic deformation $\varepsilon = 53\%$ without stress ($\sigma = 0$) after previous measurement at $\varepsilon = 100\%$; f) remaining plastic deformation $\varepsilon = 100\%$ without stress ($\sigma = 0$) after previous measurement at $\varepsilon = 195\%$. Fiber axis is vertical. Different colours correspond to different intensity ranges. Angular range (2θ) shown ranges from − 1.5 to 1.5 deg

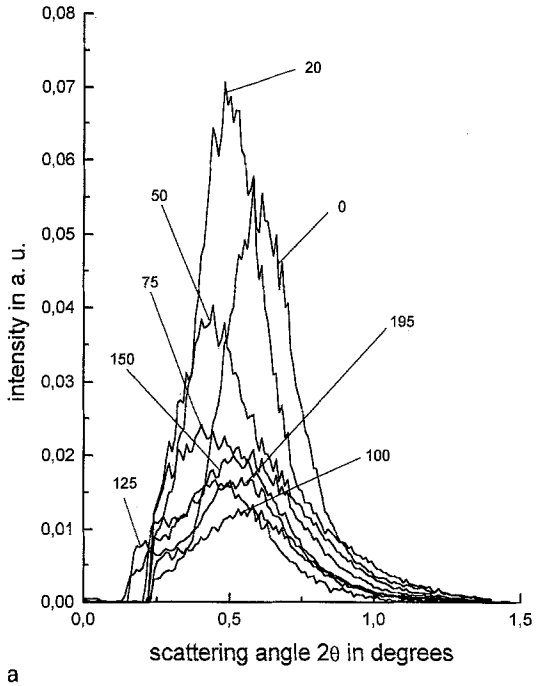

a

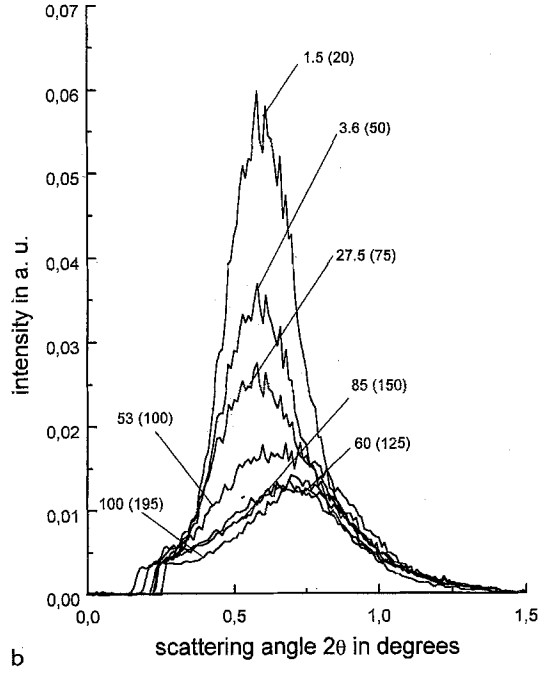

b

Fig. 2. SAXS curves of the sample obtained from the 2D pattern by meridional integration at $\chi = 90°$ taken (a) under and (b) in the absence of stress. The notation of a single number denotes the relative deformation ε, at which each measurement is carried out, whereas the plastic overall deformation is indicated by a number, followed by the previous relative deformation under stress in brackets (in percent)

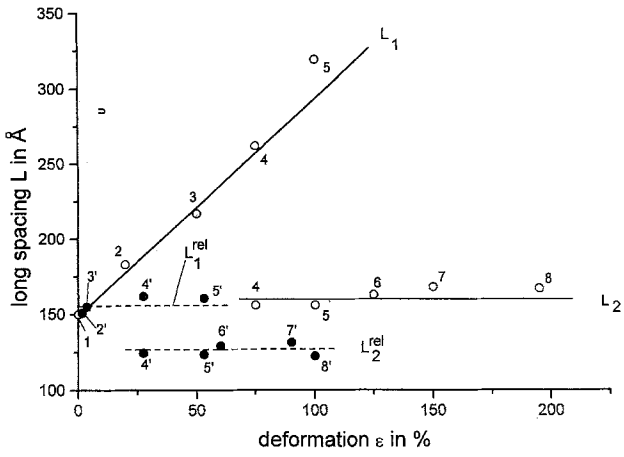

Fig. 3. Dependence of the long spacing L measured under (○) and without stress (●) on the overall relative deformation ε, at which the measurement is carried out. The primed numbers denote measurements in the absence of stress ($\sigma = 0$). The deformation ε changes as follows: 1–0%; 2–20%; 2′–1.5%; 3–50%; 3′–3.6%; 4–75%; 4′–27.5%; 5–100%; 5′–53%; 6–125%; 6′–60%; 7–150%; 7′–85%; 8–195%; 8′–100%. This plot is derived from the scattering curves shown in Fig. 2. The lines are guides for the eye

versible, and in the range $\varepsilon = 0$–100% the increase of L_1 with deformation is affine. In the deformation interval 75–100% the coexistence of two maxima in the scattering curves is observed (Fig. 4): the reflection at $\varepsilon = 75\%$ and $\varepsilon = 100\%$ has to be fitted by a superposition of two gaussian curves as indicated by the dashed lines. The solid line in Fig. 4 represents the fit and the experimental data are reasonably described. This superposition is only necessary for these two deformation states with sample PEE II, whereas in PEE I this interval was observed between 50% and 75% [1–3].

In order to get some information concerning the position of the assemblies of the parallel crystalline lamellae with respect to SD, the question of if the SAXS patterns are of two-point or four-point type should be clarified. A direct answer to this question is given by the 2D-patterns, as they are represented in Fig. 1, but a quantitative evaluation requires azimuthal scans ($\chi = 0$–180 deg) across peaks seen in Fig. 1. The results from the measurements carried out under stress are displayed in Fig. 5a, where the overall deformation ε is taken as a parameter. As can be

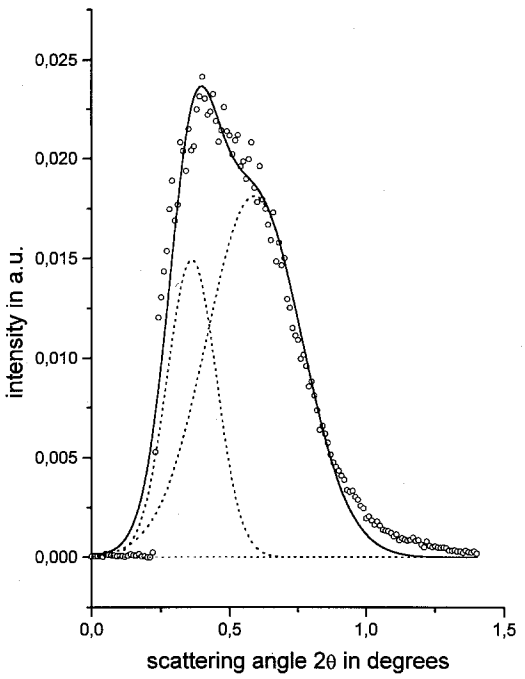

Fig. 4. Double Gaussian fit of SAXS data points obtained by meridional integration at $\chi = 90°$ for the sample at $\varepsilon = 75\%$

seen, there is only a single maximum, i.e., a two-point, 2D-pattern is always obtained. With progressing deformation ($\varepsilon = 50$–195%) this maximum flattens and decreases in intesity. In Fig. 5b azimuthal scans of the maxima in the absence of stress are presented. In this case the maximum splits with progressing plastic deformation in the range from 27.5 to 53%, which means that one deals with a four-point 2D-pattern, as can be also clearly seen in Fig. 1e for the case of residual deformation $\varepsilon = 53\%$ after a deformation of 100%.

For the description of azimuthal scans through the peaks a single gaussian fit was always attempted. This was successful for low and high deformation states, while in particular at intermediate deformation states a superposition of two plus one gaussian curves (i.e. a superposition of a four-and two-point pattern) had to be taken. This is demonstrated in Fig. 6 for the six patterns shown in Fig. 1. To obtain a reasonable fit to the azimuthal scans of the undeformed or slightly deformed samples (Fig. 6a, d) a single gaussian is sufficient, while for the relatively flat curve of $\varepsilon = 75\%$, a superposition of three gaussian curves is needed (Fig. 6b). For the relaxed sample of Fig. 6e it is also evident that two gaussians (plus a contribution of a single gaussian) have to be taken, while for the sample with $\varepsilon = 195\%$ in the stretched and relaxed state (Fig. 6c, f, respectively) the fit with one gaussian yields again a reasonable description.

Summarizing the results shown in Figs. 4–6, it is seen that at all deformation levels the 2D-SAXS patterns are of two-point type. In some of the relaxed samples ($\varepsilon = 75$–100%) the two-point patterns transform into four-point ones. In the same deformation range a second (higher-angle) component in the peak appears. One can conclude that the two-dimensional SAXS patterns in the deformation range $\varepsilon = 50$–195% are relatively complex. A detailed analysis of the 2D-scattering patterns taken under and without stress is needed to reveal underlying morphological changes of PEE materials under investigation.

Discussion

The application of SAXS for morphological characterization upon deformation is limited by the interpretation difficulties related to the complex nature of morphological changes. It is almost impossible to evaluate and distinguish the contribution to the scattering pattern of numerous structural parameters changing simultaneously during the deformation. An approach to solve this problem, particularly in the case of thermoplastic elastomers, is proposed by Pakula et al. [8, 9] who introduced a simplified model of one-dimensional assemblies of cylindrical domains arranged in a plane perpendicular to the incident x-ray beam. Further details of the model and underlying assumptions are discussed in the original papers [8, 9]. This approach was used for the morphological characterization of the structure giving rise to L_1 in a previous study on PEE I^4, and it will be applied in the present work to PEE II, too.

Let us consider the morphological behavior of PEE II as indicated by the scattering patterns. We can distinguish three deformation ranges: (i) low deformations, $\varepsilon = 0$–50%, (ii) intermediate deformations, $\varepsilon = 50$–100%, and (iii) large deformations, $\varepsilon = 100$–195%. The 2D-scattering patterns are quite different in the different regions, and also the relaxation behaviour reveals those differences.

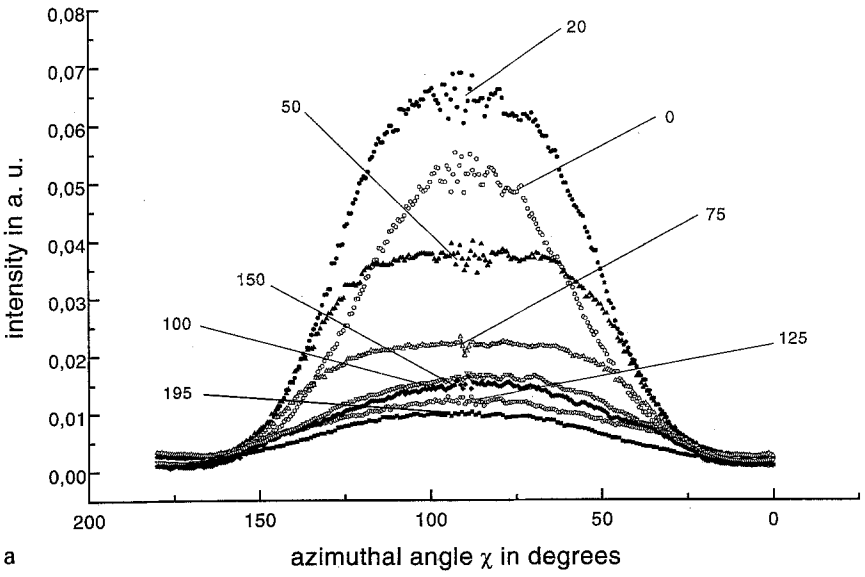

a

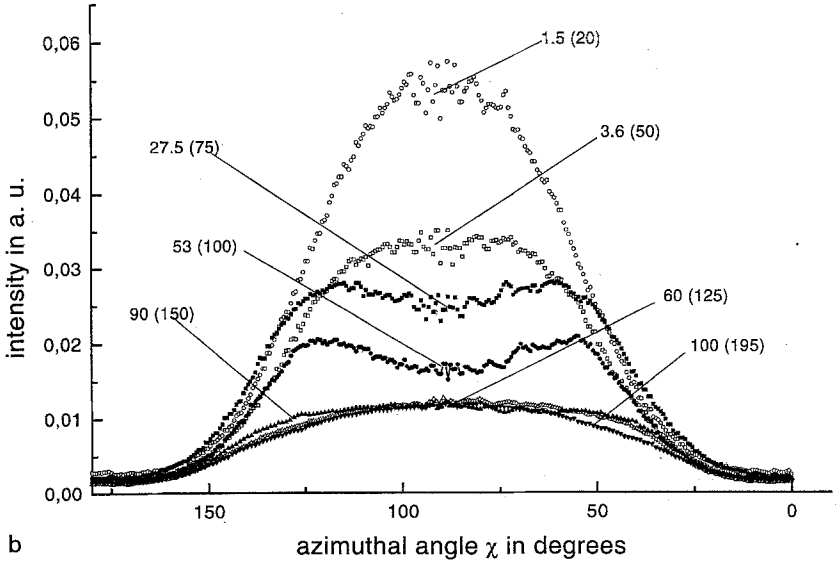

b

Fig. 5. Azimuthal scans (χ = 0–180 deg) performed at a 2θ position corresponding to the maxima obtained by meridional integration with samples (a) under and (b) without application of stress. The overall deformation measured under or without stress is indicated as parameter to each curve

In particular the intermediate regime can be viewed as a transition regime, where two morphologies coexist. In the low deformation range (up to $\varepsilon = 50\%$) the scattering curves are characterized by one maximum as shown in Figs. 1a and 2. This maximum reflects the periodicity of the crystalline lamellae created during the initial processing of the samples (drawing and annealing or vice versa) prior to the SAXS measurements and corresponds to a two-point scattering pattern in a 2D-plot as can be concluded from Fig. 1a, or from the azimuthal scans for the measurements under (Fig. 5a) or without (Fig. 5b) stress. The structure of the samples can be characterized in morphological aspect as representing assemblies of mutually parallel crystalline lamellae positioned perpendicular to SD, this arrangement remaining unchanged for both modes of measurements-under or without stress. The differences in the angular position and the intensity of the scattering peaks (Fig. 2), indicate reversible changes in the interlamellar distances (Fig. 3) as well as in the electron density difference between crystalline and amorphous regions, respectively

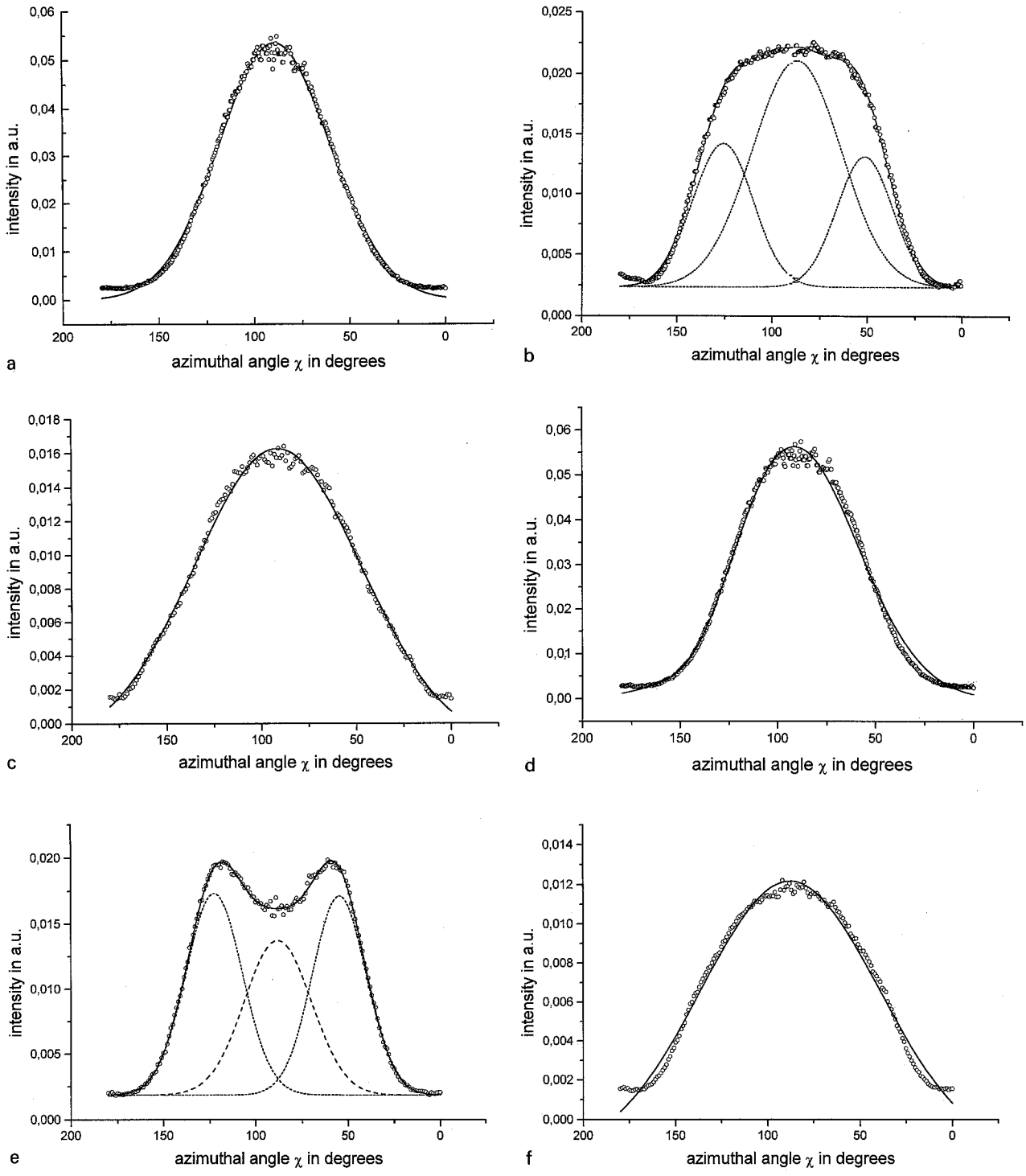

Fig. 6. Gaussian fits to data points of azimuthal scans ($\chi = 0$–180 deg) performed at the peak position for samples in different deformation states: a) $\varepsilon = 0$; b) $\varepsilon = 75\%$; c) $\varepsilon = 195\%$; d) remaining plastic deformation $\varepsilon = 1.5\%$ without stress ($\sigma = 0$) after previous measurement at $\varepsilon = 20\%$; e) remaining plastic deformation $\varepsilon = 53\%$ without stress ($\sigma = 0$) after previous measurement at $\varepsilon = 100\%$; f) remaining plastic deformation $\varepsilon = 100\%$ without stress ($\sigma = 0$) after previous measurement at $\varepsilon = 195\%$. The dashed lines indicate the individual gaussian curves, the solid lines the best overall fits to data points by a superposition of the indicated gaussian curves

[1–4]. There is a quite significant increase in peak intensity (Fig. 2a) during the first elongation ($\varepsilon = 20\%$, while the intensity then strongly decreases at $\varepsilon \geq 50\%$. It should be noted that the intensities in Fig. 2 are in an arbitrary scale, but can be compared to each other since data are corrected for the volume change of the samples during elongation. The change in intensity at low deformations is much more pronounced with PEE II as compared to PEE I [1–4] and should be related to a corresponding change in electron density contrast between crystalline and amorphous regions. Thus one can assume that first segments in the amorphous regions are extended during deformation giving rise to a drop of the density in the amorphous regions. At higher deformations also stiff sequences from the crystalline regions are pulled out, thus reducing the density of those and increasing the density of the amorphous regions again. The contrast or electron density difference is thus reduced. Based on those arguments one can also understand that the intensity after relaxation (Fig. 2b) does not reach the initial value (e.g. only approximately 80% of the initial value for $\varepsilon = 3.6\%$ after 50% elongation), while the long period essentially recovers, since those sequences cannot be incorporated into the crystalline regions again. There are, however, no indications for changes in the order of the lamellae or scattering elements with respect to SD.

Rather different is the scattering behavior of the same crystalline lamellae in the intermediate deformation range. As shown in Figs. 1b and 5a for measurements under stress, the maximum significantly broadens in azimuthal direction. For the relaxed samples in this range (Figs. 1c and 5b) in a two-dimensional presentation a four-point scattering pattern appears, indicating that the lamellae are again parallel to each other, but inclined to SD, thus forming a zigzag shaped morphology. The trend toward formation of zigzag positioned parallel lamellae is promounced only at intermediate deformation states and is valid for both states of the samples – under and without stress, as will become evident from a careful analysis of the azimutal scans over the mexima (Fig.6) – quite similar to previous observations with PEE II [4] where zigzag-shaped morphology is observed for samples with conventional and particularly with increased molecular weight but only when the sample is in its relaxed state ($\sigma = 0$).

In the intermediate deformation range ($\varepsilon = 75–100\%$) the indication of a second scattering peak, coexisting with the first one, also in meridional direction, arises. Although this peak is not very well pronounced, a single gaussian fit cannot describe the shape of the scattering curve (Fig. 4). A possibility for the appearance of the second long spacing L_2 can be the drastic shrinkage of the interlamellar distances due to the relaxation of the microfibrils as a result of loosing of interfibrillar contacts at higher deformation levels (usually above 75%) [1]. In this case L_2 remains constant with further deformation keeping a value close to the starting L_1^0 thus implicitly proving its origin [1]. This picture is consistent with the results at larger deformations discussed below, and the intermediate deformation range can be viewed as a transition region, where morphologies present at low and large deformations coexist. There are, however, other features like the zigzag-shaped lamellae, which are not significantly present in either deformation range.

Information on the morphological peculiarities of the lamellae can be gained from a more detailed analysis of the azimuthal scans of the scattering peaks (Fig. 5, 6). The intensity distribution in particular at intermediate deformations broadens and reveals a four-point fiber diagram after relaxation. One thus can conclude that the second type of lamellae which are responsible for the second periodicity L_2 in the higher deformation range morphologically can be represented as assemblies of parallel crystalline lamellae positioned perpendicular to SD. The position relative to the SD is unaffected by the loading or unloading of the sample during the SAXS measurements in the deformation range ($\varepsilon = 75–160\%$. L_2 remains constant ($L_2 = 160$ Å) at large deformations and the lamellar thickness does not change either [3, 5]. It follows that the distance between the lamellae of the seond type is insensitive to the macrodeformation in contrast to the behaviour of the lamellae of the first type.

This observation supports the assumption that the second type of periodicity arises as a result of relaxation of microfibrils after loosening some of the interfibrillar contacts due to pulling out of tie molecules. Because of the lack of interfibrillar contacts these "new" assemblies of parallel lamellae no longer participate anymore in the deformation and subsequent relaxation processes and retain their perpendicular position with respect to SD,

which is typical for the morphology of the starting structure and that of lower deformation level.

It is evident from Fig. 6 that the zigzag-shaped lamellae only appear in connection with the planar ones with both morphologies always present at the same time. The volume fraction of tilted lamellae is much larger in the relaxed samples giving rise to the four point patterns (Fig. 6b versus Fig. 6e). Also with respect to the presence of relaxed fibrils at larger deformations, which seem to be also present at intermediate deformations (Fig. 4), one might speculate that those features are connected with the loosening of contacts between fibrils. A possible model thus would include at intermediate deformation levels coexisting fibrils of different kinds: (i) affinely deformed fibrils of the original morphology containing planar lamellae of spacing L_1, (ii) relaxed fibrils, which have lost interfibrillar contacts and contain planar relaxed lamellae with spacing $L_1^{rel} = L_1^0$, and (iii) tilted lamellae, which might be originating from fibrils connecting fibrils of type (i) and (ii). They might at one side be connected by tight molecules, which are embedded in both sides, to the affinely deformed fibrils of type (i) and might have lost on the other side contact to fibrils of type (ii), which are relaxed. The deformation on one side and relaxation on the other could result in tilted lamellae. The state of deformation in the sample might be thus quite inhomogeneous along the length of a fibril, having lost contact at one place and still in contact at another. The zigzag shaped lamellae might be thus a consequence of partial break of interfibrillar contacts along fibrils and a strongly inhomogenious stress field inside the samples. This picture is supported from the results of relaxed samples, where again due to irreversible break of interfibrillar contacts and incomplete slippage of neighbouring lamellae due to partial connections by tight molecules a strong distortion of some fibrils occurs. The presence of a relatively well defined tilt angle might be explained by a balance between energies needed to pull out a chain from the neighbouring fibril followed by a slip in relation to the energy needed for a further distortion and tilt of the lamellae. This model is of course very schematic in discussing three extreme cases and intermediate states could well be possible.

At large deformations (100% to 195%) interfibrillar contacts are largely lost and the zigzag morphology does not dominate any more. In relaxed samples there is, however, still some indication of the presence of some tilted lamellae as can be seen from Fig. 6f. Here a simple gaussian fit indicated by the solid line does not give a perfect description of this azimuthal scan, but the addition of a small contribution of another two gaussians improves the fit considerably. This may be explained by the existence of a certain number of interfibrillar contacts also present for the relaxed morphology. Some tight molecules are of course still needed for mechanical strength of the material, while fibrils are largely relaxed. For PEE with increased molecular weight on the other hand the existence of a larger number of interfibrillar contacts resistant to deformation, which may be created by additional solid state reactions, can explain the presence of the zigzag-like morphology in the entire deformation range as well as the observed reversible morphological transition from zigzag shaped lamellae to smoother ones as recently reported [4].

Conclusion

In conclusion a detailed analysis of 2D x-ray scattering patterns of particular PEE materials in a large deformation range reveals the importance of interfibrillar contacts for the deformation behaviour. While the material is still affinely deformed at low elongations, interfibrillar contacts are largely lost at large deformations. In the intermediate deformation range a transition between those two morphologies is observed giving rise to a superposition of different contributions. Thus both the affinely deformed as well as the relaxed planar lamellae are present, but also tilted lamellae originating from largely deformed fibrils in an inhomogenious stress field. In the relaxed state even a four point pattern is observed. Although the deformation behaviour of PEE materials is thus relatively complex, a reasonable model can be obtained describing experimental observations.

Acknowledgements

We acknowledge the helpful discussions and suggestions by Prof. E. W. Fischer, who constantly supported this work. It is a pleasure to acknowledge the financial support provided by NATO through grant CRG 920985 and by the Bulgarian Ministry of Education and Science under contract H-216. Z. Denchev appreciates the hospitality of Max-

Planck-Institut für Polymerforschung, Mainz, where the x-ray measurements were carried out. The technical help of M. Bach during the experiments is also gratefully acknowledged.

References

1. Fakirov S, Fakirov C, Fischer EW, Stamm M (1991) Polymer 32:1173
2. Fakirov S, Fakirov C, Fischer EW, Stamm M (1992) Polymer 33:3818
3. Apostolov AA, Fakirov S (1992) J Macromol Sci Phys B31:329
4. Fakirov S, Fakirov C, Fischer EW, Stamm M, Apostolov AA (1993) Colloid Polym Sci 271:811
5. Stribeck N, Apostolov AA, Zachmann HG, Fakirov C, Stamm M, Fakirov S (1994) Int J Polym Materials 25:185
6. Gerasimov VI, Zanegin VD, Tsvankin DYa (1978) Visokomol Soedin Ser A: 20:846
7. Gerasimov VI, Zanegin VD, Smirov VD (1979) Visokomol Soedin Ser A: 21:756 (in Russian)
8. Pakula T, Saijo K, Hashimoto T (1985) Macromolecules 18:1294
9. Ibid 18:2037 (1985)
10. Legge R, Holden G, Schroeder H (1987) (eds.) "Thermoplastic Elastomers, Research and Development", Carl Hanser Verlag, Munich
11. Schroeder H, Cella RG (1988) "Polyesters, Elastomeric", in: Encyclopaedia of Polymer Science and Engineering vol 12 John Wiley & Sons, New York, Chichester, Brisbane,Toronto, Singapore
12. Wegner G (1987) "Model Studies Toward a Molecular Understanding of the Properties of Segmented Block Copolyetheresters", in: Thermoplastic Elastomers, Research and Development Legge R, Holden G, Schroeder H, (eds.) Carl Hanser Verlag, Munich
13. Droescher M, "Solid State Extrusion of Linear Polycondensates", in: Solid State Behavior of Linear Polyesters and Polyamides, Schultz JM, Fakirov S (eds.) Prentice Hall, Inc Englewood Cliffs, NJ 1990
14. Stankov S, PhD Thesis, Institute on Petrochemicals, Burgas, Bulgaria 1985
15. Gogeva T, Stankov S, Fakirov S (1990) Commun Dept Chem Bulg Acad Sci 23:377
16. Fakirov S. Gogeva T (1990) Macromol Chem 191:603

Received April 21, 1994;
accepted June 27, 1994

Authors' address:

Dr. M. Stamm
Max-Planck-Institute für Polymerforschung
Postfach 3148
55021 Mainz, FRG